**Asian Journal of Periodontics and Orthodontics**
2024, Volume 4, Page No: 98-107

Available online at: www.tsdp.net

**ISSN: 3062-3499**

**Original Article**

# Blood Cockle Shell-Derived Carbonated Hydroxyapatite-Chitosan Hydrogel for Orthodontic Stability: Post-Treatment Relapse Prevention

**Astrid Yudhit[1]*, Tubagus Ismail[1], Ummi Maimunah[2], Najmiatul Fitria[1,3]**

[1]Department of Orthodontics, Faculty of Dentistry, Universitas Gadjah Mada, Yogyakarta 55281, Indonesia.
[2]Department of Dental Biomedical Sciences, Faculty of Dentistry, Universitas Gadjah Mada, Yogyakarta 55281, Indonesia.
[3]Research Collaboration Center for Biomedical Scaffolds, National Research and Innovation Agency (BRIN), Jakarta 10340, Indonesia.

***E-mail** ✉ Yudihit.astridid@gmail.com

**Received:** 07 May 2024; **Revised:** 09 October 2024; **Accepted:** 14 October 2024

## ABSTRACT

Relapse during the retention phase of orthodontic treatment remains a considerable problem, occurring in roughly 70–90% of cases. This study investigated the potential of blood cockle shells as a natural source for producing carbonated hydroxyapatite (CHA) combined with chitosan (CS), and examined its influence on orthodontic relapse in rats. Eighteen male Wistar rats were randomly assigned into two groups: a CHA–CS group and a control group (CG). A constant orthodontic force of 35 cN was applied for 7 days, followed by a passive phase. During this period, animals in the CHA–CS group received daily applications of CHA–CS hydrogel synthesized from blood cockle shell material. Afterward, the orthodontic devices were removed to allow relapse. The mesial tip distance was measured using a digital caliper on days 1, 5, and 7 post-debonding. Histological analysis with hematoxylin–eosin (HE) staining was used to quantify osteoblasts, osteoclasts, and fibroblasts. Data were evaluated with a t-test. On day 7, the relapse distance in the CHA–CS group was significantly less than in the CG. Microscopic evaluation revealed increased osteoblast and fibroblast counts and reduced osteoclast activity during relapse ($p < 0.05$). The findings suggest that CHA–CS derived from blood cockle shells can help minimize orthodontic relapse by enhancing bone and connective tissue formation while suppressing bone resorption.

**Keywords:** Orthodontic relapse, Carbonated hydroxyapatite–chitosan hydrogel, Blood cockle shell, CHA–CS

**How to Cite This Article:** Yudhit A, Ismail T, Maimunah U, Fitria N. Blood Cockle Shell-Derived Carbonated Hydroxyapatite-Chitosan Hydrogel for Orthodontic Stability: Post-Treatment Relapse Prevention. Asian J Periodont Orthodont. 2024;4:98-107. https://doi.org/10.51847/2xhtRvV4lH

## Introduction

The popularity of cosmetic dentistry has elevated the demand for orthodontic therapy, which is now viewed as an essential aesthetic and functional procedure [1, 2]. Orthodontic treatment involves the mechanical alignment of teeth to improve facial appearance and occlusal harmony [3–5]. However, orthodontic relapse—defined as the partial or complete return of teeth toward their pre-treatment positions—remains a persistent problem due to prolonged and unstable bone remodeling processes [6–10]. The prevalence of post-treatment relapse has been estimated at 70–90%, a challenge that continues to trouble the field [11, 12]. Retention, considered the final phase of orthodontic therapy, is vital for maintaining corrected tooth positions, yet relapse can still occur even a decade after retainer removal [13, 14].

Animal studies by Franzen *et al*. [15, 16] demonstrated that alveolar bone remodeling plays a key role in relapse development. The main cellular participants—osteoclasts, osteoblasts, and fibroblasts—collectively govern this remodeling cycle. Fibroblasts regulate periodontal collagen turnover, osteoclasts resorb bone, and osteoblasts form new bone. Proper control of these interactions is essential to prevent relapse [17, 18]. Biological interventions that suppress bone resorption and stimulate bone formation have shown potential to mitigate relapse, highlighting the importance of managing alveolar

bone changes after tooth movement [19, 20]. Previous research integrating carbonated hydroxyapatite (CHA) hydrogel with advanced platelet-rich fibrin (aPRF) suggested its use as a biological retainer capable of reducing relapse risk by encouraging bone regeneration [8, 19, 21]. However, limitations such as the short lifespan of aPRF and the complex process of CHA synthesis restrict direct clinical application.

As an alternative, researchers utilized chitosan (4% w/v) and gelatin (10% w/v) hydrogels to slow orthodontic tooth movement, leveraging chitosan's versatility and biocompatibility [22, 23]. Within orthodontics, their study remains one of the few examples of chitosan used as a drug carrier. Owing to its pH sensitivity and mucoadhesive behavior at physiological pH, chitosan gel is particularly suited for intraoral application [24, 25].

Chitosan is derived from the exoskeletons of crustaceans and mollusks, including the blood cockle (Anadara granosa L.) [26, 27]. Found widely along coastal regions, cockles represent a major seafood commodity with an annual production of approximately 5200 thousand tons. Since shells constitute over 70% of total mass, at least 370 thousand tons of shell waste are generated each year [28, 29]. This accumulation contributes to environmental pollution in coastal areas. The shells, composed primarily of calcium carbonate (CaCO3) in calcite and aragonite forms [30], offer a cost-effective calcium source. CaCO3 extracted from cockle shells has proven efficient and economical for removing Pb and Cd ions from aqueous solutions [31, 32]. Recent advances in nanotechnology have focused on developing calcium carbonate nanoparticles (CSCaCO3NPs) from cockle shells as biocompatible carriers for drug delivery and as bone scaffolds. Their unique features—biocompatibility, osteoconductivity, pH responsiveness, hydrophilicity, slow degradation, and high safety profile—make them attractive for biomedical and tissue-engineering applications [33, 34].

The use of calcium hydroxyapatite (CHA) in dentistry is mainly due to its structural resemblance to natural bone and its ability to discharge calcium ions, promoting bone regeneration and remodeling processes [35]. Previous findings suggest that CHA may play a role in modulating bone turnover by enhancing osteoblast differentiation while suppressing osteoclast function. Recently, there has been growing attention toward employing chitosan (CS) to support bone repair, owing to its outstanding osteoconductive properties [36–38]. CS contributes to osteogenesis without triggering allergic responses. Moreover, CS proves highly beneficial in the regeneration of periodontal tissues because of its bioactivity, compatibility, and capacity to encourage favorable cellular reactions [39, 40]. Thus, extracting chitosan hydrogel from blood cockle shells can provide an alternative biomaterial to minimize orthodontic relapse.

The effectiveness of orthodontic treatments greatly depends on relapse prevention, a significant challenge given the widespread use of orthodontic appliances. Since large quantities of blood shells are consumed and discarded as waste, valuable components such as CHA and CS derived from them can serve to reduce relapse risk. Therefore, advancing the production of calcium hydroxyapatite–chitosan (CHA–CS) composites sourced from cockle shells could offer a promising solution for orthodontic stability. The present study aims to assess the feasibility of obtaining CHA–CS from blood cockle shells and evaluating its potential in minimizing relapse after orthodontic tooth movement.

## Materials and Methods

### *Ethical approval*

This investigation received authorization from the Ethics Committee of the Faculty of Dentistry and Prof. Soedomo Dental Hospital, Universitas Gadjah Mada, on 14 July 2023, under letter no. 131/UNI/KEP/FKG-RSGM/EC/2023.

### *Synthesis of CHA–CS from blood cockle shells*

Cockle shell powder was subjected to calcination at 800 °C for 5 h to transform $CaCO_3$ into CaO. The calcined powder was combined with $(NH_4)_2HPO_4$ and deionized water in a hydrothermal reactor and maintained at 180 °C for 20 h. The resulting hydroxyapatite was rinsed, dried, and then heated sequentially at 800 °C (1 h), 900 °C (8 h), and 1000 °C (16 h) under a $CO_2$-enriched, moisture-free atmosphere.

The conversion of chitin to chitosan followed three key stages: deproteination, demineralization, and depigmentation. For deproteination, cockle shell powder (1:10 ratio) was treated with 3.5% NaOH, stirred for 2 h at 70 °C, rinsed, and oven-dried at 60 °C. Demineralization was performed using HCl at a 1:10 (w/v) ratio, heated at 30 °C and agitated at 75 °C for 1 h. The mixture was filtered, neutralized, and dried at 60 °C. Depigmentation involved treating the demineralized sample with $H_2O_2$ at 1:10 (w/v), stirring at 50 °C for 1 h, then filtering, neutralizing, and drying at 90 °C for 2 h. To yield chitosan (CS), deacetylation was performed using 50% NaOH (1:10 w/v), heated for 2 h at 95 °C, filtered, neutralized, and dried again at 90 °C.

### *Fabrication of CHA–CS hydrogel*

A mixture of gelatin type B and CS at an 80:20 ratio was dissolved in 1% acetic acid and stirred at 60 °C for 1 h until uniform. Then, 5 g of CHA powder was added and stirred for an additional hour. Phosphoric acid ($H_3PO_4$) was diluted in 50 mL water and gradually added to the mixture, which was stirred for about 2 h until homogeneous, maintaining pH 6. The resulting gel was frozen at −18 °C for 48 h and stored at 1.7–3.3 °C.

*Fourier transform infrared spectroscopy (FTIR) analysis*

FTIR was used to characterize functional groups. The spectra were recorded using a transmission-mode FTIR at 4 $cm^{-1}$ resolution with 32 scans. CHA and CS samples were blended with KBr at a 1:100 proportion.

*Evaluation of the CHA–CS hydrogel*

Several tests were conducted to assess the hydrogel's suitability for oral mucosal application.

- *pH test*

The pH was measured before application to Wistar rat oral cavities using OneMed™ universal pH indicator strips (range 0–14). Acceptable pH levels for oral use ranged between 5.5 and 7.5.

- *Dispersion test*

A 0.5 g hydrogel sample was placed at the center of a scale paper, covered with mica, and loaded with 50 g and 100 g weights. The spread diameter was observed after 1 min until constant.

- *Contact angle test*

The contact angle was determined by placing a hydrogel droplet onto a hydrophobic surface (mica or glass). A camera positioned parallel to the surface captured the droplet image, and the angle θ between the droplet and surface was measured.

- *Organoleptic test*

Sensory evaluation of color, odor, taste, texture, and sedimentation was performed by three participants after 2 days of storage at room and chilled conditions (1.7–3.3 °C).

*Animal and experimental procedures*

This investigation employed an in vivo experimental laboratory approach using both control and treated groups of Wistar rats. The design followed that of Elkattan *et al*., who carried out a four-week protocol involving several observation periods [41, 42]. The stages were divided as follows: (1) the first week served as an acclimatization period; (2) the second week covered the placement and activation of orthodontic devices; (3) the third week involved hydrogel application for stabilization; and (4) the fourth week represented the relapse phase, during which data were collected.

A total of 18 male adult Wistar rats (Rattus norvegicus), aged 2.5–3 months and weighing 200–250 g, were selected. They were maintained in polycarbonate cages, provided with a standard pellet diet and unlimited tap water. Environmental settings were kept constant: 12-hour light/dark cycles, a temperature of 21 °C, and 50% humidity. The animals were equally allocated into control and treatment groups (nine rats each) and further randomized into three subgroups of three rats for observation on days 1, 5, and 7 after appliance removal.

Orthodontic appliances were fitted to all rats. During installation, the animals were anesthetized intramuscularly with a mixture of ketamine (10 mg/kg BW, Kepro™, Netherlands) and xylazine (Xyla™, Netherlands) in a 1:1 ratio. To achieve distal tooth movement, a three-loop spring (2 mm diameter, 6 mm length) made from 0.012″ stainless steel archwire (DiynaFlex, MO, USA) was soldered to the orthodontic band and attached to the upper incisors. The loop was activated until a 35 g force was reached, confirmed using a tension gauge (Medkraft Orthodontics, USA). This force was maintained for five days, followed by a five-day stabilization period without reactivation.

During retention, 0.1 mL of CHA–CS hydrogel was applied daily to the mesial gingival sulcus of the incisors. After five days, the appliance was removed, allowing the teeth to move naturally toward their previous positions.

*Measurement of tooth movement (Relapse distance)*

To determine relapse, the distance between the mesial edges of the upper incisors was recorded on days 1, 5, and 7 post-appliance removal using a digital caliper (0.01 mm accuracy, Pro-Max®, China). Measurements were taken twice—immediately after debonding (T0) and on the day of euthanasia (T1)—and the relapse distance was computed (T2 = T0 − T1). Each measurement was repeated three times by two independent observers blinded to the treatment conditions. A κ value of 0.89 indicated strong intra- and inter-examiner agreement, and the average of all readings was used for analysis.

*Histological processing and microscopic examination*

After appliance removal, animals were euthanized on days 1, 5, and 7 by anesthetic overdose followed by decapitation. The maxillae were dissected, fixed in 10% formalin at 4 °C for 24 h, and decalcified for 30 days in 14% EDTA (Sigma-Aldrich, USA) at pH 7.4. Samples were then dehydrated, cleared, and embedded in paraffin for 12–16 h, followed by longitudinal mesiodistal sectioning at 5 µm thickness, spaced 50 µm apart, using a Leica microtome (Model 819, Germany).

Sections were stained using hematoxylin–eosin (H&E) to visualize osteoblasts, osteoclasts, and fibroblasts. Deparaffinization involved immersing slides in xylol twice for 3 min each, followed by rehydration through graded alcohol and water. Samples were stained with hematoxylin (6–7 min), rinsed under water (1 min), followed by eosin staining (3 min) and another series of washes with 70% alcohol and water. Finally, slides were mounted with Entellan® and covered with glass slips.

Histological analysis focused on the mesial (pressure) side of relapse. Five random regions of interest (ROIs) were examined, from cervical to apical bone regions, using a light microscope (OptiLAB LLC Phoenix, USA) at 400×

magnification. Cell counts were performed using Image Raster 3.0® (USA). Two independent examiners, each repeating analyses thrice, achieved strong agreement (κ = 0.88).

- Osteoclasts appeared as multinucleated cells with pink cytoplasm near Howship's lacunae.
- Osteoblasts were cuboidal, with single dark blue–purple nuclei, lining the bone surface.
- Fibroblasts were spindle-shaped with flattened oval nuclei, identified in the periodontal ligament. Active fibroblasts were recognized by distinct cytoplasm, smooth chromatin, and clear morphology. The mean cell count across the five ROIs for each incisor was recorded as the representative value.

*Statistical analysis*

All results were analyzed using parametric statistical methods. Data distribution was assessed by the Shapiro–Wilk test and Levene's homogeneity test at a 95% confidence level ($p > 0.05$). Comparisons between groups were conducted using an independent t-test, considering a significance level of $p < 0.05$.

**Results and Discussion**

*Formation of CHA and chitosan from blood cockle shells*

Before producing CHA and chitosan, the blood cockle shells were first finely milled in a ball grinder and sieved through a 100-mesh screen. From an initial 2 kg of raw shells, approximately 346 g (±35%) of 100-mesh powder was obtained. Using 50 g of this powder, the CHA synthesis produced 30 g (±60%) of a fully carbonated A-type hydroxyapatite. Likewise, another 50 g batch yielded 20 g (±40%) of chitosan.

*FTIR characterization of CHA and chitosan derived from blood shells*

Functional group identification of CHA compounds was carried out using FTIR spectroscopy. The spectrum in **Figure 1** displays peaks at 3642.50 and 604.66 cm−1, corresponding to OH− stretching, while an OH− hydration signal appeared at 3437.74 cm−1. A mild band at 1420.14 cm−1 was attributed to CO32− group vibrations, signifying atmospheric carbonate incorporation on the surface of hydroxyapatite particles. During chemical precipitation, CO2 presence may promote carbonate substitution for hydroxyl or phosphate groups. Absorption signals at 1080.37 and 1038.26 cm−1 were linked to PO43− units, verifying that pure CHA was successfully formed. The FTIR outcomes for CHA are presented in **Table 1**.



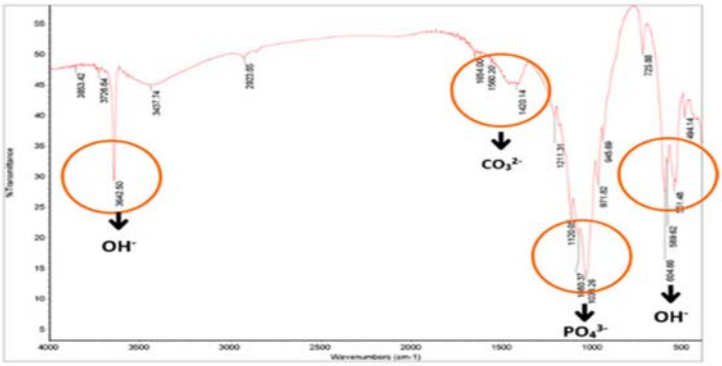


**Figure 1.** FTIR spectra of the analyzed materials. The red marks highlight OH−, CO32−, and PO43− absorption regions associated with blood cockle shell–derived CHA.

**Table 1.** FTIR results for CHA obtained from blood cockle shells.

| Bond Type | Wavenumber ($cm^{-1}$) of Blood Cockle Shell Hydroxyapatite | Wavenumber ($cm^{-1}$) of Hydroxyapatite from Literature [43] |
|---|---|---|
| Hydroxyl ($OH^-$) | 3642.50 and 604.66 | 3575 |
| Hydrated OH | 3437.74 | 3423 |
| Carbonate ($CO_3^{2-}$) | 1420.14 | 1470–1420 |
| Phosphate ($PO_4^{3-}$) | 1080.37 and 1038.26 | 1085–1092 |

To confirm the conversion of chitin to chitosan, FTIR spectroscopy was also applied. **Figure 2** illustrates the FTIR spectrum of the synthesized chitosan. The broad absorption around 3404.63 cm−1 corresponds to overlapping OH− and N–H stretching, indicating deacetylation. The 2925.36 cm−1 peak represents C–H stretching from alkanes, linked to –CH2– vibrations. The diminished C=O peak (1651.00 cm−1) compared to that of chitin suggests successful transformation. Additionally, the presence of C–N amine absorption at 1420.29 cm−1 and C–O vibration at 1155.02 cm−1 confirms the structure of chitosan. The FTIR findings are summarized in **Table 2**.

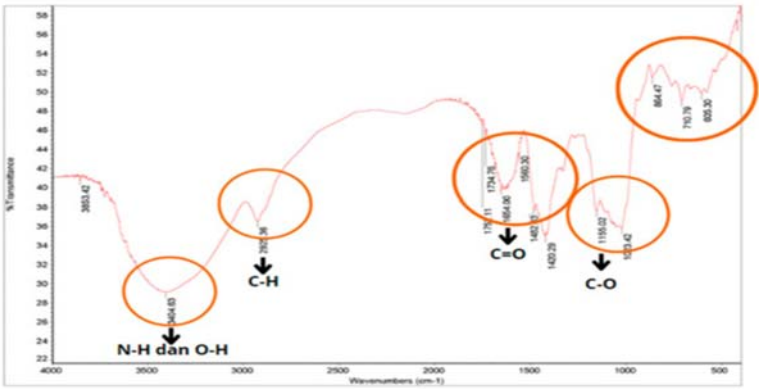


**Figure 2.** FTIR spectrum of chitosan from blood cockle shells, showing absorption peaks corresponding to N–H, O–H, C–H, C=O, and C–O groups.

**Table 2.** FTIR data for synthesized chitosan.

| Bond Type | Wavenumber ($cm^{-1}$) of Chitosan from Blood Cockle Shell | Wavenumber ($cm^{-1}$) of Chitosan Hydroxyapatite from Literature [44] |
|---|---|---|
| N-H bond | 3404.63 | 3500–3100 |
| O-H bond | 3404.63 | 3400–3200 |
| C-H bond | 2925.36 | 3000–2850 |
| C=O bond | 1651.00 | 1654–1541 |
| C-N amine bond | 1420.29 | 1400 |
| C-O bond | 1155.02 | 1200–1180 |



*Hydrogel formulation assessment*

*pH measurement*

The measured pH of the resulting hydrogel was 6 **(Table 3)**. A pH between 5.5 and 6.6 typically enhances adhesive capacity, as confirmed by rheological observations showing that greater compression increases gel firmness and viscosity. Elevated viscosity reinforces molecular cohesion during application, ensuring better spreading and retention of the hydrogel on oral mucosa while minimizing washout from saliva [45, 46].

**Table 3.** pH measurement of the hydrogel.

| Day | 0 | 1 | 3 |
|---|---|---|---|
| pH test results | 6 | 6 | 6 |

*Spreadability evaluation*

For the dispersion study, 0.5 mL of hydrogel was pipetted onto grid paper, producing a spread radius of 0.35 mm from the center, equivalent to a 0.7 mm total diameter.

*Contact angle determination*

The contact angle test, shown in **Figure 3**, distinguished between hydrophilic and hydrophobic surfaces using θ = 90° as a threshold. A smaller angle corresponds to stronger hydrophilicity, while a larger one indicates hydrophobic behavior. The CHA–CS hydrogel exhibited a 72° angle on a hydrophobic substrate, which is below 90°, signifying hydrophilic nature—consistent with prior literature [47].

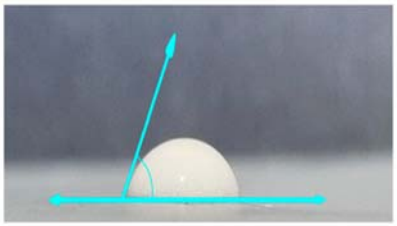

**Figure 3.** Contact angle analysis of CHA–CS hydrogel droplets. The blue reference line marks the interface between the base surface and the droplet slope, showing θ = 72°.

*Organoleptic observation*

The organoleptic assessment was performed following two days of storage, and the results are summarized in **Table 4**. Samples maintained under cold conditions demonstrated a milder odor, a cloudy white hue, a slightly sweet–sour taste, and a thick, gel-like consistency, with visible sedimentation occurring after more than 30 minutes of standing. Conversely, specimens kept at ambient temperature developed a stronger scent, a clearer white appearance, a sweet–sour taste, and a thinner, more fluid texture, with precipitation beginning in under 20 minutes. Variations in temperature are known to influence the hydrogel's sensory traits—such as flavor, color, texture, and sedimentation rate [48].

**Table 4.** Organoleptic evaluation results.

| Condition | Odor | Appearance | Flavor | Texture | Sedimentation Time |
|---|---|---|---|---|---|
| Cold Temperature | Less intense | Opaque white suspension | Sweet–sour | Firm gel | >30 min |
| Room Temperature | More intense | Transparent white suspension | Sweet–sour | Fluid gel | <20 min |

*Relapse distance and histological findings*

Measurements of relapse distance were conducted on days 1, 5, and 7 following debonding. Throughout the observation period, animals treated with the formulation exhibited shorter relapse distances compared to the untreated controls **(Figure 4)**. The histological comparison between both groups is displayed in **Figure 5**, showing distinct tissue responses. **Table 5** lists the mean values and standard deviations for relapse distances and the cellular counts of osteoclasts, osteoblasts, and fibroblasts in both the treated and control groups (using CHA–CS hydrogel). A statistically significant decrease in osteoclast number was found in the experimental group on day 5 post-debonding. In contrast, osteoblast numbers were markedly higher in the CHA–CS group by day 7. Additionally, fibroblast counts were consistently greater on days 1, 5, and 7 in the treated samples than in controls after orthodontic relapse ($p < 0.05$).

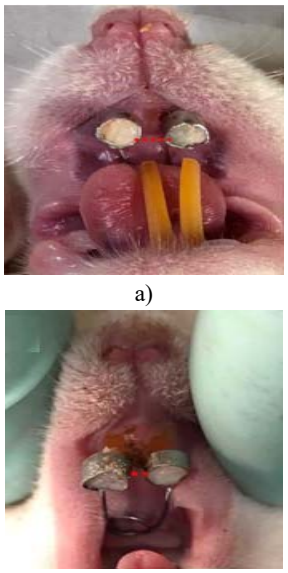

a)

b)

**Figure 4.** Comparison of relapse distances between groups after seven days of observation. Application of CHA–CS hydrogel a) minimized relapse in the experimental group b) relative to controls.



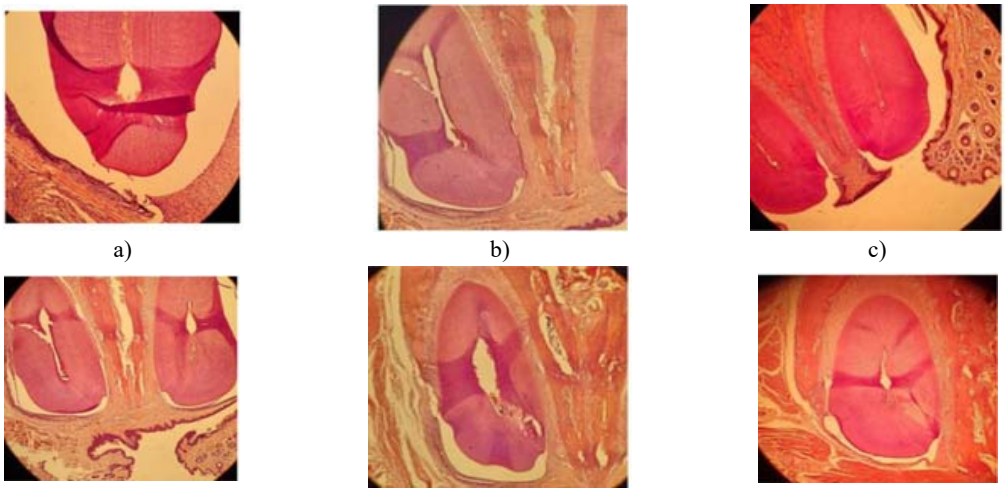

a) b) c)

d) e) f)

**Figure 5.** Microscopic appearance of upper incisors. The upper panels represent control group specimens at 1, 5, and 7 days after debonding, while the lower panels depict the CHA–CS hydrogel group at identical intervals (400× magnification).

**Table 5.** Statistical results (mean ± SD) and t-test comparisons for relapse distance (mm) and counts of osteoblasts, osteoclasts, and fibroblasts (cells/field) between groups on days 1, 7, and 14 after debonding.

| Parameter | CHA-CS Group | Control Group | p-Value |
|---|---|---|---|
| **Relapse Distance (mm)** | | | |

| | | | |
|---|---|---|---|
| Day 0 | 1.13 ± 0.58 | 0.75 ± 0.05 | 0.105 |
| Day 5 | 0.85 ± 0.09 | 0.77 ± 0.31 | 0.507 |
| Day 7 | 0.75 ± 0.05 | 0.80 ± 0.30 | 0.790 |
| **Osteoblast Count** | | | |
| Day 1 | 24.80 ± 5.59 | 20.61 ± 1.82 | 0.179 |
| Day 5 | 21.34 ± 1.87 | 17.06 ± 3.41 | 0.076 |
| Day 7 | 26.68 ± 3.72 | 18.14 ± 2.71 | 0.004 * |
| **Osteoclast Count** | | | |
| Day 1 | 2.80 ± 0.27 | 2.81 ± 0.45 | 0.699 |
| Day 5 | 1.29 ± 0.45 | 2.31 ± 0.57 | 0.025 * |
| Day 7 | 1.32 ± 0.27 | 2.22 ± 0.84 | 0.095 |
| **Fibroblast Count** | | | |
| Day 1 | 13.63 ± 3.41 | 8.21 ± 3.11 | 0.032 * |
| Day 5 | 13.12 ± 2.53 | 7.20 ± 2.77 | 0.016 * |
| Day 7 | 12.81 ± 2.33 | 6.20 ± 1.79 | 0.008 * |

p-value < 0.05: indicates significant intergroup differences.

Modern tissue engineering approaches are being explored to control alveolar bone remodeling, minimize orthodontic relapse, and maintain tooth alignment. Carbonate apatite (CHA) has emerged as a promising biomaterial in bone tissue regeneration because of its controlled calcium ion release and osteogenic capability [49]. The current results demonstrated a clear rise in osteoblast populations within the CHA–CS hydrogel–treated specimens. CHA enhances bone repair by elevating local calcium and phosphate concentrations—key elements for mineralized tissue formation. The secretion of these ions into surrounding tissues modulates osteoblast function while limiting osteoclast differentiation. Increased extracellular calcium supports osteoblastic DNA synthesis and chemotactic activity while suppressing osteoclastogenesis [8, 50]. Moreover, CHA promotes the expression of transforming growth factor-β1 (TGF-β1) and bone morphogenetic protein-2 (BMP-2), both of which are essential for osteoblast differentiation. TGF-β1 not only encourages osteoblast precursor recruitment and matrix synthesis but also prevents apoptosis of mature osteoblasts. This growth factor additionally contributes to collagen production and fibroblast proliferation, thereby facilitating bone matrix formation and regeneration [19].

The findings revealed a marked rise in fibroblast counts within the treated specimens. Yamamoto *et al*. were among the first to report that transcription factors such as Runx2, Osterix, Oct3/4, and L-Myc (RXOL) could be utilized to directly reprogram fibroblasts into osteoblasts [51]. Since osteoblasts are essential for new bone generation, transforming fibroblasts into osteoblasts represents a potential method for promoting bone repair. Both osteoblasts and osteoclasts are central to the biological mechanisms regulating orthodontic relapse, being responsible for bone synthesis and resorption. During the relapse phase, the side that initially underwent tension during tooth movement becomes the pressure side. This shift results in enhanced osteoclast differentiation and bone degradation. Conversely, the original pressure side becomes the tension side, encouraging osteoblast differentiation and stimulating bone deposition [8, 20, 22].

In animals treated with CHA–CS, the osteoclast count was noticeably reduced. Mechanistically, CHA supports bone remodeling by increasing the local concentration of calcium and phosphate ions. Higher extracellular calcium levels are known to encourage osteoblast proliferation and migration while simultaneously hindering osteoclast development [52]. Previous evidence has demonstrated that elevated phosphate levels can suppress osteoclast formation by increasing osteoprotegerin (OPG) synthesis and by inducing osteoclast apoptosis directly [53]. A reduction in osteoclast activity has been associated with slower orthodontic tooth movement [54]. The use of CHA may therefore prevent relapse by enhancing OPG expression and reducing receptor activator of nuclear factor-κB ligand (RANKL) levels. These results imply that local CHA application can effectively inhibit osteoclastogenesis and activity, thereby improving orthodontic stability [8]. OPG, a natural receptor secreted by osteoblasts, limits osteoclast differentiation by binding RANKL and preventing its interaction with the receptor activator of nuclear factor kappa-B (RANK). When RANKL interacts with RANK, hematopoietic precursor cells rapidly differentiate into mature osteoclasts [55].

A further advantage of CHA lies in its potential role as a carrier in controlled drug delivery systems [56]. A major challenge in tissue engineering is achieving precise delivery for bone regeneration. Controlled release systems are beneficial because they can convert low–molecular weight substances into higher–

molecular weight structures, thereby minimizing degradation before therapeutic action occurs. Gelatin-based hydrogels were selected in this study due to their favorable water regulation, biodegradability, and ability to enable sustained release through cross-linking. Enzymatic breakdown of gelatin hydrogels generates soluble gelatin fragments, facilitating the gradual release of encapsulated bioactive materials [57].

One limitation of the current work was the use of hematoxylin–eosin (HE) staining to identify and quantify osteoclasts, osteoblasts, and fibroblasts. This manual counting method can introduce subjectivity. Future research should incorporate specific biomarkers to objectively confirm the quantities of these cells and strengthen the study's conclusions.

## Conclusion

The synthesis of CHA and CS from blood cockle shells was confirmed through FTIR analysis, demonstrating consistent functional group patterns. Several characteristics of the developed hydrogel were identified: a pH of 6, a contact angle of 72° reflecting hydrophilic nature, a dispersion diameter of 0.7 cm, and favorable organoleptic stability under cold storage conditions. In a seven-day in vivo relapse experiment, CHA–CS hydrogel derived from blood cockle shells was found to significantly reduce orthodontic relapse by elevating osteoblast and fibroblast levels while diminishing osteoclast numbers. Further studies are recommended to assess different concentrations of the carbonate hydroxyapatite–chitosan hydrogel from blood cockle shells and to evaluate its clinical applicability in human orthodontic therapy.

**Acknowledgments:** None

**Conflict of Interest:** None

**Financial Support:** None

**Ethics Statement:** None

## References

1. Indriasari V, Suparwitri S, Christnawati C, Alhasyimi AA. Different effects of soybean isoflavone genistein on transforming growth factor levels during orthodontic tooth movement among young and old rabbits. F1000Research. 2019;8(2074):1–9.
2. Egwunatum AE, Uyovbisere E, Umeh LC. Effect of Forest-Incubated Composts on Crude-oil Soils for Zea mays, L. Cultivation in Delta State, Nigeria. World J Environ Biosci. 2022;11(3):14-20. doi: 10.51847/j5Pyls0seh
3. Alam MK, Kanwal B, Abutayyem H, Alswairki HJ, Alfawzan AA, Shqaidef A, et al. Complications arising due to orthodontic treatment—A systematic review and meta-analysis. Appl Sci (Basel). 2023;13(7):4035.
4. Petronis Z, Pliatkute I, Janovskiene A, Leketas M. The Relationship Between Cervical Spine Abnormalities and Temporomandibular Joint Internal Disorders: A Systematic Review of Literature. Ann Dent Spec. 2023;11(4):20-8. doi:10.51847/sGUN5P9OQA
5. Maiti S, Rai N, Appanna P, Jessy P. Digital Telescopic Denture- A Viable Treatment Modality of Preventive Prosthodontics: Clinical Report. Ann Dent Spec. 2022;10(4):1-4. doi:10.51847/eEgUl0vYgd
6. Kalina E, Grzebyta A, Zadurska M. Bone remodeling during orthodontic movement of lower incisors—Narrative review. Int J Environ Res Public Health. 2022;19(23):15002.
7. Rosyida NF, Ana ID, Alhasyimi AA. The use of polymers to enhance post-orthodontic tooth stability. Polymers (Basel). 2023;15(1):103.
8. Alhasyimi AA, Pudyani PP, Asmara W, Ana ID. Enhancement of post-orthodontic tooth stability by carbonated hydroxyapatite-incorporated advanced platelet-rich fibrin in rabbits. Orthod Craniofac Res. 2018;21(2):112–8.
9. Karpov VY, Medvedev IN, Komarov MN, Puchkova NG, Sharagin VI, Petina ES. The Influence of Regular Physical Activity on the Functional Parameters of the Youthful Organism. J Biochem Technol. 2023;14(2):18-23. doi:10.51847/QB2dBXs8ij
10. Nguyen DT, Hoang TH. The Influence of Organizational Capabilities on Operational Efficiency: A Study of Vietnamese Businesses. Asian J Indiv Organ Behav. 2022;2:15-20. doi:10.51847/PapKxH2ZYU
11. Kaan M, Madléna M. Retenció és recidiva az ortodonciában. Irodalmi áttekintés (Retention and relapse. Review of the literature). Fogorv Sz. 2011;104(4):139–46.
12. Alshammari E. Efficacy of Generic vs. branded Isotretinoin for Acne treatment: a case report. J Adv Pharm Educ Res. 2021;11(1):125-7. doi:10.51847/UvTeFaq1oI
13. Al Yami EA, Kuijpers-Jagtman AM, van't Hof MA. Stability of orthodontic treatment outcome: Follow-up until 10 years postretention. Am J Orthod Dentofacial Orthop. 1999;115(3):300–4.
14. Alharthi NS. Endocannabinoid system components: A crucial role in regulation of disease. J Adv Pharm

Educ Res. 2022;12(3):72-81. doi:10.51847/FIVP7AOddG

15. Franzen TJ, Monjo M, Rubert M, Vandevska-Radunovic V. Expression of bone markers, and micro-CT analysis of alveolar bone during orthodontic relapse. Orthod Craniofac Res. 2014;17(4):249–58.
16. Satushieva L, Isakov A, Maremkulova R, Tekueva M, Zalikhanova L. Some Peculiarities of Administrative Penalties System and the Order of Their Imposition in Russia. J Organ Behav Res. 2021;6(2):100-8. doi:10.51847/DnsGazKwqt
17. Martin TJ. Bone biology and anabolic therapies for bone: Current status and future prospects. J Bone Metab. 2014;21(1):8–20.
18. Elgendy TYAAA. Evaluating Internal Auditor Selection through Analytical Network Process: A Case Study Approach. Ann Organ Cult Leadersh Extern Engagem J. 2023;4:35-44. doi:10.51847/K4wmaJTGng
19. Alhasyimi AA, Suparwitri S, Christnawati C. Effect of carbonate apatite hydrogel-advanced platelet-rich fibrin injection on osteoblastogenesis during orthodontic relapse in rabbits. Eur J Dent. 2021;15(3):412–419.
20. Lin Y, Fu ML, Harb I, Ma LX, Tran SD. Functional biomaterials for local control of orthodontic tooth movement. J Funct Biomater. 2023;14(6):294.
21. Sergun V, Gorbushina I, Valentina B, Poznyakovsky V, Tokhiriyon B, Lapina V. Exploring the Efficacy of a Novel Lake Salt-Based Supplement for Primary Dysmenorrhea. Spec J Pharmacogn Phytochem Biotechnol. 2022;2:27-31. doi:10.51847/LKDf0jzmER
22. Montero Jiménez OG, Dib Kanán A, Dipp Velázquez FA, Aristizábal Pérez JF, Moyaho Bernal MdLA, Salas Orozco MF, et al. Use of hydrogels to regulate orthodontic tooth movement in animal models: A systematic review. Appl Sci (Basel). 2022;12(13):6683.
23. Drobotova AN, Filippova VV, Ovechko OY, Leshchenko YY, Belova PS, Tabukhova AZ. Postpartum Bleeding: Definition, Diagnostic Approaches, and Management Protocols in Contemporary Research. Interdiscip Res Med Sci Spec. 2023;3(2):31-5. doi:10.51847/ShO1maIzLU
24. Asefi S, Seifi M, Fard GH, Lotfi A. Innovative evaluation of local injective gel of curcumin on the orthodontic tooth movement in rats. Dent Res J (Isfahan). 2018;15(1):40–9.
25. Yang J, Tang Z, Shan Z, Leung YY. Integrating Rapid Maxillary Expansion and Le Fort Osteotomy for Esthetic Rehabilitation: A Clinical Case Report. J Curr Res Oral Surg. 2023;3:22-6. doi:10.51847/E0OEwI52jo
26. Prado HJ, Matulewicz MC. Cationization of polysaccharides: A path to greener derivatives with many industrial applications. Eur Polym J. 2014;52(1):53–75.
27. Duangthip D, Gao SS, Chen KJ, Lo ECM, Chu CH. Investigating the Relationship between Oral Health Related Life Quality and the Severity of Dental Caries in Children. Turk J Dent Hyg. 2023;3:22-8. doi:10.51847/hRLJbKoNZM
28. Chalermwat K, Szuster BW, Flaherty M. Shellfish aquaculture in Thailand. Aquac Econ Manag. 2003;7(5–6):249–261.
29. Hassan F, Hatah E. An Analytical Exploration of Various Non-Pharmacological Approaches Utilized in Managing Diabetes Among Patients in Malaysia. Int J Soc Psychol Asp Healthc. 2022;2:27-37. doi:10.51847/JmKuHOeBQX
30. Xu Z, Valeo C, Chu A, Zhao Y. The efficacy of whole oyster shells for removing copper, zinc, chromium, and cadmium heavy metal ions from stormwater. Sustainability (Basel). 2021;13(8):4184.
31. Panpho P, Vittayakorn N, Sumang R. Synthesis, scrutiny, and applications of bio-adsorbents from cockle shell waste for the adsorption of Pb and Cd in aqueous solution. Crystals (Basel). 2023;13(4):552.
32. Khalil AM. Advances in Epigenome Engineering: Mastering Technical Approaches for Better Outcomes. J Med Sci Interdiscip Res. 2023;3(2):21-34. doi:10.51847/iBbxxQHVQH
33. Muhammad Mailafiya M, Abubakar K, Danmaigoro A, Musa Chiroma S, Bin Abdul Rahim E, Aris Mohd Moklas M, et al. Cockle shell-derived calcium carbonate (aragonite) nanoparticles: A dynamite to nanomedicine. Appl Sci (Basel). 2019;9(14):2897.
34. Mashhour K, Saad E, Abdelghany H, Hashem W. Acute Toxicity Comparison between 3DCRT and SIB-IMRT in Preoperative Concurrent Chemo-Radiotherapy for Locally Advanced Rectal Cancer. Arch Int J Cancer Allied Sci. 2023;3(2):16-24. doi:10.51847/PVlZaAgP9c
35. Pajor K, Pajchel L, Kolmas J. Hydroxyapatite and fluorapatite in conservative dentistry and oral implantology: A review. Materials (Basel). 2019;12(17):2683.
36. Ishikawa K, Hayashi K. Carbonate apatite artificial bone. Sci Technol Adv Mater. 2021;22(1):683–94.
37. Chen C, Chang N, Wu Y, Fu E, Shen E, Feng C, et al. Bone formation using cross-linked chitosan scaffolds in rat calvarial defects. Implant Dent. 2018;27(1):15–21.
38. Nasr AMA, Ahmed YAM, Gafar AAM, Ahmed SAD, Barri BKA, Meshref ET, et al. A Systematic Review of the Prevalence and Risk Factors Associated with Choriocarcinoma in Saudi Arabia.

Asian J Curr Res Clin Cancer. 2022;2(1):18-24. doi:10.51847/YkmsatQnNJ

39. Shetty C, Shetty A, Shetty S, Kaur G, Hegde MN, Nidhi L. Applications of chitosan in dentistry. Indian J Public Health Res Dev. 2020;11(2):99–105.
40. Mohey M, Soliman H, Okasha A. The Potential Role of CD31 in Type 2 Diabetes Mellitus, an Initial Investigation. Ann Pharm Pract Pharmacother. 2021;1:1-8. doi:10.51847/8qAI1cGTvD
41. Elkattan AE, Gheith M, Fayed MS, El Yazeed MA, Farrag AH, Khalil WKB. Effects of different parameters of diode laser on acceleration of orthodontic tooth movement and its effect on relapse: An experimental animal study. Maced J Med Sci. 2019;7(3):412–20.
42. Grin NA, Platova EG, Dukaev MV, Magomedovic AM, Gairbekov MK, Sulimanova KI, et al. Evaluating the Effectiveness of Silver Nanoparticle-Modified Dental Fillings on Enhancing Hard Tissue Durability. Int J Dent Res Allied Sci. 2023;3(2):29-35. doi:10.51847/XdLVg7zuuq
43. Abifarin JK, Obada DO, Dauda ET, Dodoo-Arhin D. Experimental data on the characterization of hydroxyapatite synthesized from biowastes. Data Brief. 2019;26(1):104485.
44. Sayyidah NA, Darjati, Suryono H. The examination of the quality of chitosan from bamboo shell waste with variations of NaOH concentration in the deacetylation process. Int Conf Environ Health (ICoEH). 2021;1(1):71–9.
45. Maslii Y, Ruban O, Kasparaviciene G, Kalveniene Z, Materiienko A, Ivanauskas L, et al. The influence of pH values on the rheological, textural, and release properties of carbomer. Molecules (Basel). 2020;25(22):5018.
46. Covello F, Ruoppolo G, Carissimo C, Zumbo G, Ferrara C, Polimeni A, et al. Study of Quality of Life Associated with Oral Health in Patients with MS (Multiple Sclerosis). Ann J Dent Med Assist. 2021;1(2):17-23. doi:10.51847/JddDeasVKr
47. Alghunaim A, Kirdponpattara S, Newby BZ. Techniques for determining contact angle and wettability of powders. Powder Technol. 2016;287(1):201–15.
48. Wang Y, Burgess DJ. Influence of storage temperature and moisture on the performance of microsphere/hydrogel composites. Int J Pharm. 2013;454(1):310–5.
49. Fujioka-Kobayashi M, Tsuru K, Nagai H, Fujisawa K, Kudoh T, Ohe G, et al. Fabrication and evaluation of carbonate apatite-coated calcium carbonate bone substitutes for bone tissue engineering. J Tissue Eng Regen Med. 2018;12(9):2077–87.
50. Anitua E, de la Fuente M, Troya M, Zalduendo M, Alkhraisat MH. Autologous platelet-rich plasma (PRGF) preserves genomic stability of gingival fibroblasts and alveolar osteoblasts after long-term cell culture. Dent J (Basel). 2022;10(9):173.
51. Yamamoto K, Kishida T, Sato Y, Nishioka K, Ejima A, Fujiwara H, et al. Direct conversion of human fibroblasts into functional osteoblasts by defined factors. Proc Natl Acad Sci U S A. 2015;112(19):6152–6157.
52. Wu X, Itoh N, Taniguchi T, Nakanishi T, Tanaka K. Requirement of calcium and phosphate ions in expression of sodium-dependent vitamin C transporter 2 and osteopontin in MC3T3-E1 osteoblastic cells. Biochim Biophys Acta. 2003;1641(1):65–70.
53. Kanatani M, Sugimoto T, Kano J, Kanzawa M, Chihara K. Effect of high phosphate concentration on osteoclast differentiation as well as bone-resorbing activity. J Cell Physiol. 2003;196(1):180–189.
54. Jindarojanakul C, Chanmanee P, Samruajbenjakun B. Analysis of osteoclasts and root resorption in corticotomy-facilitated orthodontics with ibuprofen administration—An animal study. Dent J (Basel). 2022;10(9):170.
55. D'Apuzzo F, Cappabianca S, Ciavarella D, Monsurrò A, Silvestrini-Biavati A, Perillo L. Biomarkers of periodontal tissue remodeling during orthodontic tooth movement in mice and men: Overview and clinical relevance. Sci World J. 2013;2013(1):105873.
56. Maarof NNN, Abdulmalek E, Fakurazi S, Rahman MBA. Biodegradable carbonate apatite nanoparticle as a delivery system to promote afatinib delivery for non-small cell lung cancer treatment. Pharmaceutics. 2022;14(6):1230.
57. Saito T, Tabata Y. Preparation of gelatin hydrogels incorporating low-molecular-weight heparin for anti-fibrotic therapy. Acta Biomater. 2012;8(2):646–52.